



ARCHIVES  
of  
FOUNDRY ENGINEERING

ISSN (2299-2944)  
Volume 18  
Issue 1/2018

71 – 76

DOI: 10.24425/118814

13/1



Published quarterly as the organ of the Foundry Commission of the Polish Academy of Sciences

# The Microstructure and Properties of the Bimetallic AZ91/AlSi17 Joint Produced by Compound Casting

R. Mola \*, T. Bucki

Kielce University of Technology

al. Tysiąclecia Państwa Polskiego 7, 25-314 Kielce, Poland

\* Corresponding author. E-mail address: rmola@tu.kielce.pl

Received 20.06.2017; accepted in revised form 24.08.2017

## Abstract

Bimetallic AZ91/AlSi17 samples were produced by compound casting. The casting process involved pouring the AZ91 magnesium alloy heated to 650°C onto a solid AlSi17 aluminum alloy insert placed in a steel mould. Prior to casting, the mould with the insert inside was heated to about 370°C. The bonding zone formed between AZ91 and AlSi17 had a thickness of about 200 µm; it was characterized by a non-homogeneous microstructure. Two different areas were distinguished in this zone: the area adjacent to the AZ91 and the area close to the AlSi17. In the area closest to the AZ91 alloy, a eutectic composed of an Mg<sub>17</sub>Al<sub>12</sub> intermetallic phase and a solid solution of Al in Mg was observed. In bonding zone at a certain distance from the AZ91 alloy an Mg<sub>2</sub>Si phase co-occurred with the eutectic. In the area adjacent to the AlSi17 alloy, the structure consisted of Al<sub>3</sub>Mg<sub>2</sub>, Mg<sub>17</sub>Al<sub>12</sub> and Mg<sub>2</sub>Si. The fine Mg<sub>2</sub>Si phase particles were distributed over the entire Mg-Al intermetallic phase matrix. The microhardness of the bonding zone was much higher than those of the materials joined; the microhardness values were in the range 203-298 HV. The shear strength of the AZ91/AlSi17 joint varied from 32.5 to 36 MPa.

**Keywords:** Innovative foundry technologies and materials, Compound casting process, Bonding zone, Microstructure, Mechanical properties

## 1. Introduction

As magnesium alloys are known to exhibit many attractive properties, including low density, high specific strength, good workability and good castability, their applications are numerous. They are increasingly used for structural elements in the automotive, aerospace and electronics industries. The main drawback of Mg alloys is that they have poor surface properties, especially low hardness and low resistance to wear and corrosion. Surface modification is therefore essential. Many surface treatment methods can be used [1]. Surface alloying with Al is a common technique employed to improve the surface properties of

Mg-based materials [2-7]. Fabrication of bimetallic Al/Mg parts with an Al surface layer is another solution to this problem. Al and Al alloys are characterized by good corrosion resistance. When Al is used as the surface layer of an Mg-based component, its corrosion resistance is improved while the density is kept low. This is of importance in the transport sector. Different methods can be used to join these two types of materials, for instance, hot pressing [8], hot rolling [9,10], extrusion [11,12], explosive cladding [13] and twin-roll casting [14]. Compound casting is another method employed to join different metals or alloys [15-17]; it has been applied to produce lightweight Mg-Al components. In this process, one metal or alloy is directly cast onto a solid insert made of the other metal placed in a mould. The

literature dealing with this method discusses the joining of Mg to AlMg1 aluminum alloy [18], Mg to Al [19-21] and AZ91 magnesium alloy to AlSi17 aluminum alloy [22,23]. An interesting aspect of bimetal fabrication is the mechanical behavior of the bonding zone.

This article analyses the microstructure and properties of the bimetallic joint between AZ91 and AlSi17 produced by compound casting. The microhardness and shear strength of the joint were examined to determine its mechanical behavior.

## 2. Experiment

The AZ91 magnesium alloy and the AlSi17 aluminum alloy were used as the cast material and the solid insert, respectively. The composition of the AZ91 alloy was as follows: 9.14% Al, 0.64% Zn, 0.23% Mn (wt%). AlSi17 alloy was composed of 17.18% Si, 1.22% Mg, 0.82% Ni, 0.72% Cu, 0.25% Fe and 0.02% Zn with a balance of Al. To fabricate the AZ91/AlSi17 bimetallic samples, cylindrical inserts, 30 mm in diameter and 10 mm in thickness, were cut from rapidly solidified AlSi17 alloy. The surface of the insert was ground with silicon carbide papers up to 800 grit; then, the insert was placed at the bottom of a steel mould. The mould with an insert inside was heated up to about 370°C. The AZ91 alloy was melted under pure argon atmosphere. The casting process was performed under normal atmospheric conditions. It involved top-pouring 100 grams of molten AZ91 at 650°C onto the AlSi17 insert placed in the mould. A schematic diagram of the compound casting process is shown in Fig. 1.

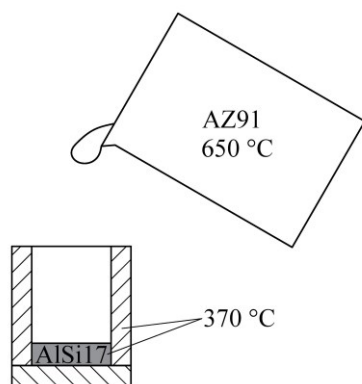


Fig. 1. Schematic illustration of the compound casting process

After casting, the AZ91/AlSi17 samples were cut in the longitudinal direction. Five bimetallic specimens were fabricated and analyzed. In four of the five cases, the results were repeatable. In one of the specimens, discontinuities of the bonding zone were reported locally. The microstructure of the bonding zone was examined in all the bimetallic specimens over the entire cross-section. The microstructural investigations were conducted with a Nikon ECLIPSE MA 200 optical microscope and a JEOL JSM-5400 scanning electron microscope. The chemical composition of the bonding zone was analyzed using an X-ray energy dispersive spectrometer (EDS) attached to the SEM. The structural constituents of the bonding zone were identified through

quantitative SEM-EDS analysis on the basis of the binary Al-Mg [24] and ternary Al-Mg-Si [25] phase diagrams.

The microhardness of both alloys and the bonding zone between them was measured with a MATSUZAWA MMT Vickers hardness tester under a load of 100 g. The shear strength of the AZ91/AlSi joint was determined using a LabTest5.20SP1 universal testing machine at a displacement of 10 mm/min. Shear tests were performed for six specimens. The lowest and highest values of shear strength are provided. As pure shear is a stress state that is difficult to achieve, simple shear tests were carried out. In a simple shear test, large tangential stresses occur together with small normal stresses due to bending or tension. Simple shear is assumed to be a case of shear when a uniform shear stress state is observed in a cross-section, with bending stresses being negligible. A schematic diagram of the simple shear test setup is illustrated in Fig. 2.

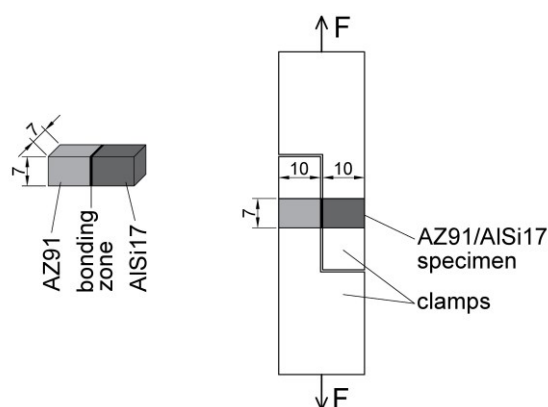


Fig. 2 Schematic diagram of the simple shear test

## 3. Results and discussion

Figure 3 shows an optical microscopic image of the microstructure of the bonding zone between the AZ91 magnesium alloy and the AlSi17 aluminum alloy produced by compound casting. The bonding zone, about 200  $\mu\text{m}$  in thickness, was characterized by a nonhomogeneous microstructure. Two different areas can be distinguished in this zone: one adjacent to AZ91 and the other adjacent to AlSi17 (marked A and B, respectively).

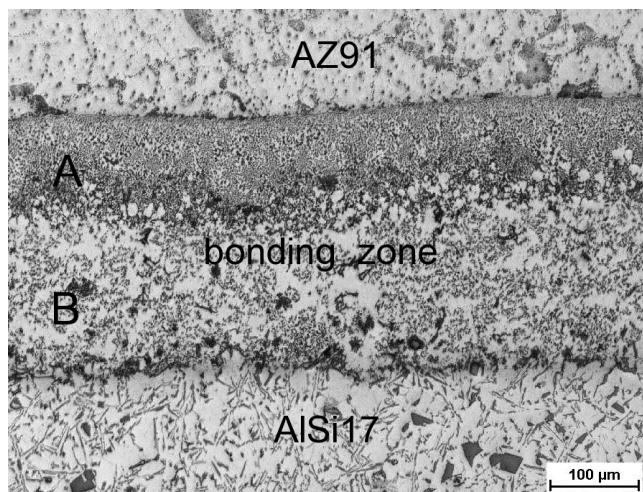


Fig. 3. Microstructure of the bonding zone formed by compound casting between AZ91 and AlSi17

Figures 4 and 5 show the microstructures of the bonding zone near the AZ91 alloy and the AlSi17 alloy, respectively; the corresponding EDS line scan results showing the concentration profiles of the elements present (Mg, Al and Si) are also included.

As shown in Fig. 4, there is a two-phase structure in the bonding zone near the AZ91 alloy. The results of the EDS quantitative analysis conducted at four selected points (Fig. 4) are provided in Table 1. The EDS line scan results indicate a high concentration of Al in the light areas (point 1) of the two-phase structure. The chemical composition of these areas indicates an  $Mg_{17}Al_{12}$  intermetallic phase. The results of the quantitative analysis conducted for the dark phase (point 2) suggest a solid solution of Al in Mg. From the phase equilibrium diagram for Mg-Al [24] it is clear that this two-phase structure is a eutectic composed of an  $Mg_{17}Al_{12}$  phase and a solid solution of Al in Mg. The light dendrites (point 3) observed close to the eutectic are also the  $Mg_{17}Al_{12}$  intermetallic phase. Near the dendrites, there are agglomerates of dark, fine particles (point 4). A high concentration of Si was detected in this area. The quantitative analysis for a dark particle (point 4) suggests the  $Mg_2Si$  phase. The EDS profile of the Si distribution along the index line indicates that the agglomerates of these particles are also present in the eutectic area near dendrites. The results are in agreement with the literature data [25]; the analysis of the Mg-Al-Si ternary system revealed that the structural constituents of magnesium-rich alloys are: a solid solution of Al in Mg, an  $Mg_{17}Al_{12}$  intermetallic phase and an  $Mg_2Si$  phase.

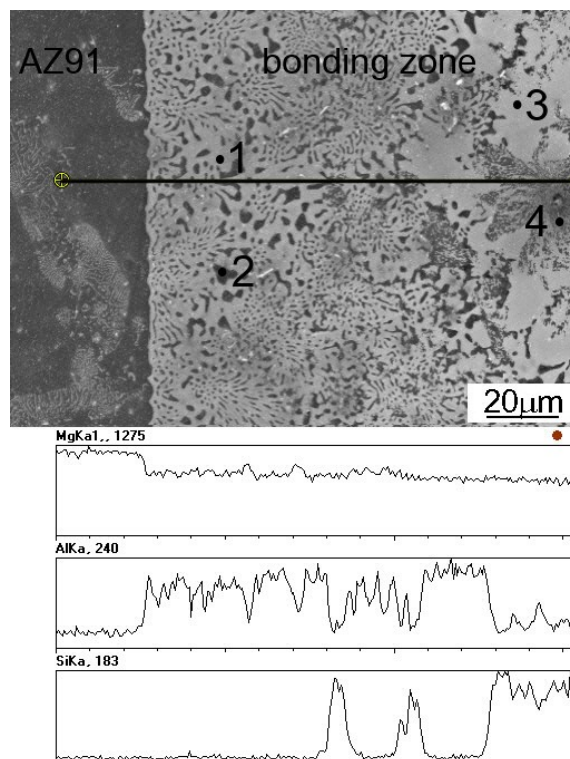


Fig. 4. Microstructure of the bonding zone close to the AZ91 alloy (area marked A in Fig. 3) with a distribution of elements (Mg, Al and Si) along the marked line

Table 1.

Results of the EDS quantitative analysis at points marked in Fig. 4

Point	Mg	Al	Si
		at. %	
1	62.47	37.53	-
2	91.58	8.42	-
3	61.89	38.11	-
4	66.89	3.73	29.38

The distribution of elements along the line marked in Fig. 5 confirms the presence of Si primary crystals and eutectic Si in the AlSi17 aluminum alloy near the bonding zone. These structural constituents were not detected in the bonding zone close to the AlSi17. In the bonding zone there are dark particles over the light matrix. Figure 6 shows details of the microstructure of this zone. The results of the EDS quantitative analysis at points 1-3 (Fig. 6) are given in Table 2. As can be seen, the light matrix is non-homogeneous; lighter and darker areas (marked 1 and 2, respectively) can be distinguished. The chemical composition of the lighter areas is similar to that of the  $Al_3Mg_2$  intermetallic phase, whereas the composition of the darker regions resembles that of the  $Mg_{17}Al_{12}$  intermetallic phase. The dark particles present in the bonding zone are distributed irregularly. Locally, they occur as agglomerates. The chemical composition of these agglomerates (marked 3) is close to that of the  $Mg_2Si$  phase. Previous studies by the authors [22,23] indicated that the use of an AlSi17 insert cut from an ingot with coarse primary Si crystals

resulted in the occurrence of Si particles in the bonding zone, which had not fully reacted during the casting process. In this study, the insert material was the AlSi17 alloy after thermal modification. As can be seen from Fig. 3, there are no Si particles in the bimetallic joint. This suggests that the Si particles in the insert material were fine; during compound casting, they reacted with Mg and were fully transformed into the Mg<sub>2</sub>Si phase.

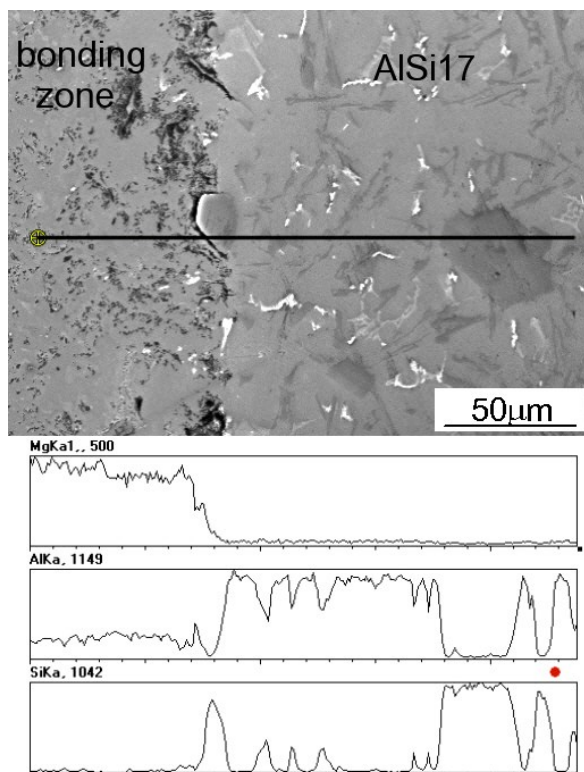


Fig. 5. Microstructure of the bonding zone close to the AlSi17 alloy (area marked B in Fig. 3) with a distribution of elements (Mg, Al and Si) along the marked line

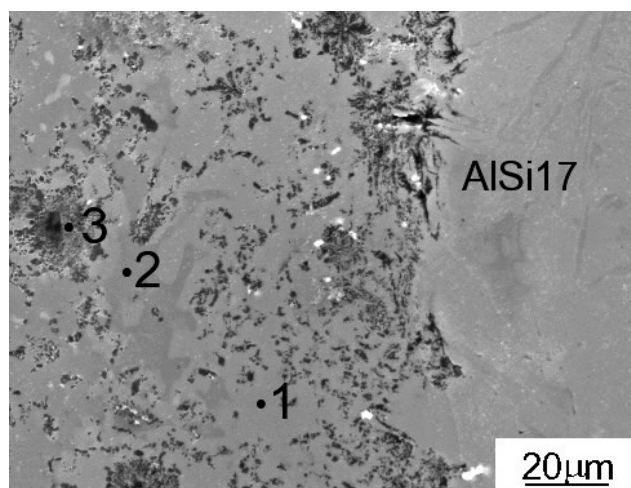


Fig. 6. Microstructure of the bonding zone close to the AlSi17 alloy with points of the EDS quantitative analysis

Table 2.

Results of the EDS quantitative analysis at points marked in Fig. 6

Point	Mg	Al	Si
	at. %		
1	39.50	60.50	-
2	60.25	39.75	-
3	68.90	1.4	29.7

The formation of the bonding zone between AZ91 and AlSi17 during compound casting is assumed to have proceeded as follows. The casting involved pouring liquid AZ91 heated to 650 °C onto a solid AlSi17 insert heated to 370 °C. The higher temperature of the molten material resulted in partial melting of the insert surface. The thin layer of the melt formed between the solid AlSi17 insert and the solidifying AZ91 alloy was enriched with the elements present in both alloys. The interdiffusion of the elements at the interface led to the formation of new phases with melting points lower than those of the two alloys. After casting, the temperature at the AZ91/AlSi17 reactive interface lowered and the liquid solidified. A continuous transition zone formed between the two materials. The microstructure of the zone was not homogeneous because of the concentration gradient along the reactive interface. In the area adjacent to the AZ91, a eutectic microstructure (an Mg<sub>17</sub>Al<sub>12</sub> intermetallic phase + a solid solution of Al and in Mg) was observed. At a certain distance from the AZ91 alloy, the Mg<sub>2</sub>Si phase co-occurred with the eutectic. In the area close to the AlSi17, Mg<sub>2</sub>Si particles were found in the Mg-Al intermetallic phase matrix.

Figure 7 shows indentations left by the Vickers penetrator in the AZ91 alloy, the bonding zone and the AlSi17 alloy and the corresponding microhardness values. The results show that the microhardness of the bonding zone is much higher than those of the alloys joined. The highest microhardness values were reported in the area close to the AlSi17 alloy. In this case, the bonding zone was composed of fine Mg<sub>2</sub>Si particles distributed over the matrix consisting of the Mg-Al intermetallic phases. As shown in [21], the microhardness values obtained for the Mg<sub>17</sub>Al<sub>12</sub> and Al<sub>3</sub>Mg<sub>2</sub> phases were 220-228 HV and 250-256 HV, respectively. The hardness of the Mg<sub>2</sub>Si phase (450 HV [26]) is higher than those of the Mg-Al intermetallic phases. In the eutectic close to the AZ91 alloy, the microhardness values were lower. The constituents of this two-phase structure were: a hard Mg<sub>17</sub>Al<sub>12</sub> phase and a soft solid solution of Al in Mg.

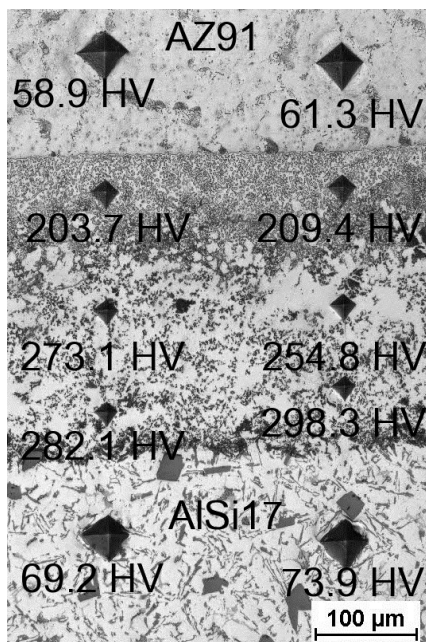


Fig. 7. Microhardness indentations in the bonding zone and the materials joined

The average shear strength of the joint in the AZ91/AISi17 bimetallic samples ranged from 32.5 to 36 MPa. The damage mechanism for all the shear specimens was similar. Figure 8 shows a fractured sample with a crack in the bonding zone close to the AISi17 alloy propagating parallel to the interface. The fracture occurred in the zone composed of fine  $Mg_2Si$  phase particles distributed over the Mg-Al intermetallic phase matrix. The fracture seems to be due to the brittleness of the hard Mg-Al intermetallic phases [27] constituting the matrix of the bonding zone close to the AISi17 alloy.

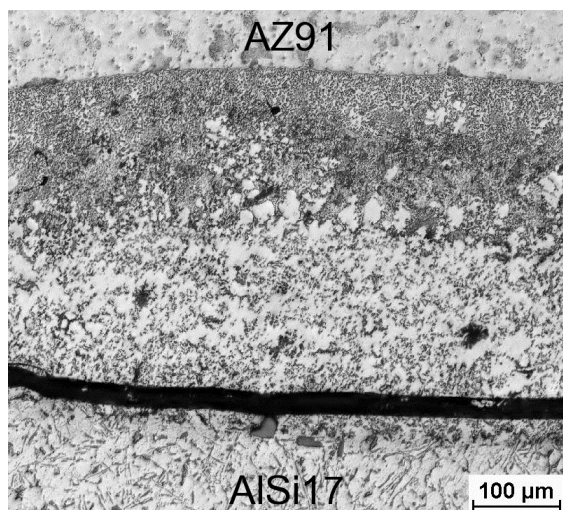


Fig. 8. Shear fractured specimen

The results of the shear tests presented here are in agreement with the results available in the literature concerning the

properties of this type of bonding zone containing Mg-Al intermetallic phases. In [20], the authors determined the shear strength of the bonding zone between Mg and Al formed by compound casting using push-out tests. The shear strength of the bonding zone ranged from 8.3 MPa to 27 MPa, depending on its thickness. It was found that a decrease in the shear strength of the bonding zone was due to an increase in its thickness and, consequently, an increase in the amount of brittle and very hard  $Al_3Mg_2$  and  $Mg_{17}Al_{12}$  intermetallic phases.

## 4. Conclusions

The bimetallic AZ91/AISi17 samples were fabricated by compound casting. The bonding zone between the alloys with a thickness of about 200  $\mu m$  was characterized by a nonhomogeneous microstructure. In the area close to the AZ91 magnesium alloy, a eutectic (an  $Mg_{17}Al_{12}$  intermetallic phase + a solid solution of Al and in Mg) was observed. At a certain distance from the AZ91 alloy an  $Mg_2Si$  phase co-occurred with the eutectic. In the area adjacent to the AISi17 aluminum alloy, fine  $Mg_2Si$  particles over the Mg-Al intermetallic matrix were reported. The microhardness of the bonding zone was several times higher than those of the materials bonded; the microhardness values ranged from 203 to 298 HV. The shear strength of the joint varied between 32.5 and 36 MPa.

## References

- [1] Gray, J.E. & Luan, B. (2002). Protective coatings on magnesium and its alloys – a critical review. *Journal of Alloys and Compounds*. 336(1-2), 88-113.
- [2] Ignat, S., Sallamand, P., Grevey, D. & Lambertin, M. (2004). Magnesium alloys laser (Nd:YAG) cladding and alloying with side injection of aluminium powder. *Applied Surface Science*. 225(1), 124-134.
- [3] Singh, A. & Harimkar, S.P. (2012). Laser surface engineering of magnesium alloys: a review. *JOM*. 64(6), 716-733.
- [4] Dziadoń, A., Mola, R. & Błaż, L. (2016). The microstructure of the surface layer of magnesium laser alloyed with aluminium and silicon. *Materials Characterization*. 118, 505-513.
- [5] Shigematsu, M., Nakamura, M., Saitou, K. & Shimojima, K. (2000). Surface treatment of AZ91D magnesium alloy by aluminum diffusion coating. *Journal of Materials Science Letter*. 19(6), 473-475.
- [6] Mola, R. (2015). The properties of Mg protected by Al- and Al/Zn-enriched layers containing intermetallic phases. *Journal Materials Research*. 30(23), 3682-3691.
- [7] Taha, M.A., El-Mahallawy, N.A., Hammouda, R.M. & Nassef, S.I. (2010). PVD Coating of Mg-AZ31 by thin layer of Al and Al-Si. *Journal of Coatings Technology and Research*. 7(6), 793-800.
- [8] Zhu, B., Liang, W. & Li, X. (2011). Interfacial microstructure, bonding strength and fracture of magnesium-aluminium laminated composite plates fabricated by direct

- hot pressing. *Materials Science and Engineering: A*. 528(21), 6584-6588.
- [9] Zhang, X.P., Yang, T.H., Castagne, S. & Wang, J.T. (2011). Microstructure; bonding strength and thickness ratio of Al/Mg/Al alloy laminated composites prepared by hot rolling. *Materials Science and Engineering: A*. 528(4), 1954-1960.
- [10] Wierzba, A., Mróz, S., Szota, P., Stefanik, A. & Mola, R. (2015). The influence of the asymmetric ARB process on the properties of Al-Mg-Al multi-layer sheets. *Archives of Metallurgy and Materials*. 60(4), 2821-2825.
- [11] Liu, X.B., Chen, R.S. & Han, E.H. (2009). Preliminary investigation on the Mg-Al-Zn/Al laminated composite fabricated by equal channel angular extrusion. *J. Mater. Process. Tech.* 209(10), 4675-4681.
- [12] Binotsch, C., Nickel, D., Feuerhack, A. & Awiszus, B. (2014). Forging of Al-Mg compounds and characterization of interface. *Procedia Engineering*. 81, 540-545.
- [13] Mróz, S., Stradomski, G., Dyja, H. & Galka, A. (2015). Using the explosive cladding method for production of Mg-Al bimetallic bars. *Archives of Civil and Mechanical Engineering*. 15(2), 317-323.
- [14] Bae, J.H., Prasada Rao, A.K., Kim, K.H. & Kim, N.J. (2011). Cladding of Mg alloy with Al by twin-roll casting. *Scripta Materialia*. 64(9), 836-839.
- [15] Wróbel, T. & Szajnar, J. (2015). Bimetallic casting: ferritic stainless steel-grey cast iron. *Archives of Metallurgy and Materials*. 60(3), 2361-2365.
- [16] Wróbel, T., Cholewa, M. & Tenerowicz, S. (2011). Bimetallic layered castings alloy steel – carbon cast steel. *Archives of Foundry Engineering*. 11(1), 105-108.
- [17] Szymczak, T. (2011). The influence of selected technological factors on the quality of bimetallic castings alloy steel-silumin. *Archives of Foundry Engineering* 11(3), 215-226.
- [18] Papis, K.J.M., Loeffler, J.F. & Uggowitzer, P.J. (2009). Light metal compound casting. *Science in China Series E: Technological Sciences*. 52(1), 46-51.
- [19] Hajjari, E., Divandari, M., Razavi, S.H., Homma, T. & Kamado, S. (2012). Intermetallic compounds and antiphase domains in Al/Mg compound casting. *Intermetallics*. 23, 182-186.
- [20] Emami, S.M., Divandari, M., Arabi, H. & Hajjari, E. (2013). Effect of melt-to-solid insert volume ratio on Mg/Al dissimilar metals bonding. *Journal of Materials Engineering and Performance*. 22(1), 123-130.
- [21] Mola, R., Bucki, T. & Dziadoń, A. (2016). Formation of Al-alloyed layer on magnesium with use of casting techniques. *Archives of Foundry Engineering*. 16(1), 112-116.
- [22] Mola, R., Bucki, T. & Dziadoń, A. (2017). Effects of the pouring temperature on the formation of the bonding zone between AZ91 and AlSi17 in the compound casting process. *IOP Conference Series: Materials Science and Engineering*. 179(1), 1-6.
- [23] Mola, R., Bucki, T. & Dziadoń, A. (2017). Microstructure of the bonding zone between AZ91 and AlSi17 formed by compound casting. *Archives of Foundry Engineering*. 17(1), 202-206.
- [24] Crystallographic and Thermodynamic Data of Binary Alloys, Landolt-Börnstein New Series, Group IV, Springer-Verlag Berlin 1998.
- [25] Tang, Y., Du, Y., Zhang, L., Yuan, X. & Kaptay, G. (2012). Thermodynamic description of the Al-Mg-Si system using a new formulation for the temperature dependence of the excess Gibbs energy. *Thermochim. Acta*. 527, 131-142.
- [26] Westbrook, J.H. & Fleischer, R.L. (2000). *Structural applications of intermetallic compounds*. John Wiley & Sons.
- [27] Hayat, F. (2011). The effects of the welding current on heat input, nugget geometry, and the mechanical and fractural properties of resistance spot welding on Mg/Al dissimilar materials. *Materials & Design*. 32(4), 2476-2484.